HYDROLOGICAL PROCESSES
Hydrol. Process. **13**, 1935–1959 (1999)

A spatially distributed energy balance snowmelt model for application in mountain basins

Danny Marks,[1]* James Domingo,[2] Dave Susong,[3] Tim Link,[2] and David Garen[4]

[1]*USDA Agricultural Research Service, Northwest Watershed Research Center, 800 Park Blvd., Suite 105, Boise, ID 83712, 208/422-0721, USA*

[2]*Oregon State University, EPA National Health and Environmental Effects Research Lab., Corvallis, OR 97333, 541/754-4452, USA*

[3]*US Geological Survey, Utah District, Salt Lake City, UT 84104, 801/975-3397, USA*

[4]*USDA National Resource Conservation Service, National Water and Climate Center, Portland, OR 97204-3224, 503/414-3021, USA*

Abstract:

Snowmelt is the principal source for soil moisture, ground-water re-charge, and stream-flow in mountainous regions of the western US, Canada, and other similar regions of the world. Information on the timing, magnitude, and contributing area of melt under variable or changing climate conditions is required for successful water and resource management. A coupled energy and mass-balance model ISNOBAL is used to simulate the development and melting of the seasonal snowcover in several mountain basins in California, Idaho, and Utah. Simulations are done over basins varying from 1 to 2500 km^2, with simulation periods varying from a few days for the smallest basin, Emerald Lake watershed in California, to multiple snow seasons for the Park City area in Utah. The model is driven by topographically corrected estimates of radiation, temperature, humidity, wind, and precipitation. Simulation results in all basins closely match independently measured snow water equivalent, snow depth, or runoff during both the development and depletion of the snowcover. Spatially distributed estimates of snow deposition and melt allow us to better understand the interaction between topographic structure, climate, and moisture availability in mountain basins of the western US. Application of topographically distributed models such as this will lead to improved water resource and watershed management. Copyright © 1999 John Wiley & Sons, Ltd.

KEY WORDS spatially distributed modelling; snowmelt; runoff; water resources

INTRODUCTION

Water from melting snow is a critical resource in the western US, Canada, and other similar regions of the world. To address the need for improved management of this resource, we present an energy balance snowmelt runoff model, that is explicitly distributed over a digital representation of topographic structure, represented by a digital elevation model (DEM). This model has been under development for the past decade, first described by Marks (1988), Marks *et al.* (1992), and Marks and Dozier (1992). Application of the point version of the model SNOBAL was presented by Marks *et al.* (1998), Link (1998), and Link and Marks (1999, this issue).

The model follows from the work of Anderson (1976) who showed that it was possible to accurately simulate the energy balance of a snowcover to predict snowmelt. He concluded, however, that such models were too complicated, consuming far too much of the then limited computer resources, and requiring forcing data that were seldom available at an experimental site, much less over a watershed or region (Anderson,

* Correspondence to: USDA Agricultural Research Service, Northwest Watershed Research Center, 800 Park Blvd., Suite 105, Boise, ID 83712, 208/422-0721, USA.

CCC 0885–6087/99/121935–25$17·50

Received 3 June 1998
Revised 1 February 1999
Accepted 18 March 1999

1979). He correctly predicted that operational forecasting would rely on lumped parameter, spatially averaged snowmelt models for some time to come.

In the period that followed, several groups continued to develop energy balance snowmelt models as research tools. All of these involved some level of parameterization of the forcing inputs, the physics of the energy balance, or the spatial distribution across the topographic structure of the site, basin, watershed, or region. Those models that retain accurate representation of the physics of the energy balance and detail of snowcover structure have been limited to point applications or simulations over small experimental sites. The SNTHERM model (Jordan, 1991) accurately simulates snowcover energy and mass balance, but requires extensive forcing and snowcover structure data. SNTHERM also requires the input of snow structure and conditions, during deposition events, so it has difficulty simulating the development of the snowcover, unless detailed deposition data are available. Flerchinger and Saxton (1989) developed and used the SHAW model to simulate the energy and mass balance of the soil and snowcover as a system. This model accurately represents the processes involved, but is too complicated to explicitly distribute over a grid. Flerchinger *et al.* (1994) used the SHAW model in point mode, to do multiple simulations over a small drainage, showing that if you could distribute a physically based model, it could provide detailed information on how spatially and temporally varying snowmelt impacts basin hydrology and soil moisture. Tarboton *et al.* (1995, 1996) show that both snow deposition and ablation can be simulated, but their Utah energy balance model (UEB) is too complicated for a distributed application over areas larger than a few hectares. In general, only the more parameterized models have been widely applied over mountain drainages. The USGS PRMS model (Leavesley *et al.*, 1983, 1987) is one such model that has extensively parameterized the critical energy exchange processes, and is only quasi-distributed, relying on a limited number of topographic zones. Though it can be applied over larger drainages and basins, its limited representation of complex hydrologic processes leaves much to be desired (Risley *et al.*, 1997).

The snowcover energy and mass-balance model (SNOBAL) presented in this paper accurately represents the physics of the snowcover energy balance and snowmelt, and has been shown to accurately represent both the development and ablation of the snowcover during a wide range of climate and snowcover conditions, and geographic locations (Marks *et al.*, 1998). The grid based, spatially distributed version of this model, ISNOBAL, is explicitly distributed over a DEM grid. The successful development and implementation of this model has been possible to a large extent because of the numerical efficiency of the software tool system that it is part of. Both the point (SNOBAL) and image (ISNOBAL) versions of the model are part of the Image Processing Workbench (IPW) software system, originally developed by Frew (1990), modified by Longley and Marks (1991) and Longley *et al*, (1992) and then extensively expanded and updated by Marks, Domingo, and Frew (1999). Development and testing of the model has also relied on the continued cost reduction and very rapid improvement in computer speed and storage capacity.

In both sections below we present examples of simulation of the development and melting of the seasonal snowcover in mountain basins in California, Idaho, and Utah. These simulations were done over basins varying from 1 to 10 000 km^2, with simulation periods varying from a few weeks for the smallest basin, to multiple snow seasons for the largest basin. These examples represent a chronology of the development of this model, showing how it closely follows improvements in low-cost desktop computer workstations. The final test represents probably the first grid-based simulation of the snowcover energy and mass balance over a high resolution DEM grid (75 m) representing a significantly large region, at high temporal resolution (hourly) for multiple snow seasons. This test includes both the development and ablation of the snowcover, and results indicate that the model accurately represents snowcover processes during both low and high snowcover conditions.

MODEL DESCRIPTION

The model ISNOBAL is a DEM grid-based energy balance snowmelt model that uses initial conditions describing the snowcover, topographic structure of the region, and measurement heights, with distributed

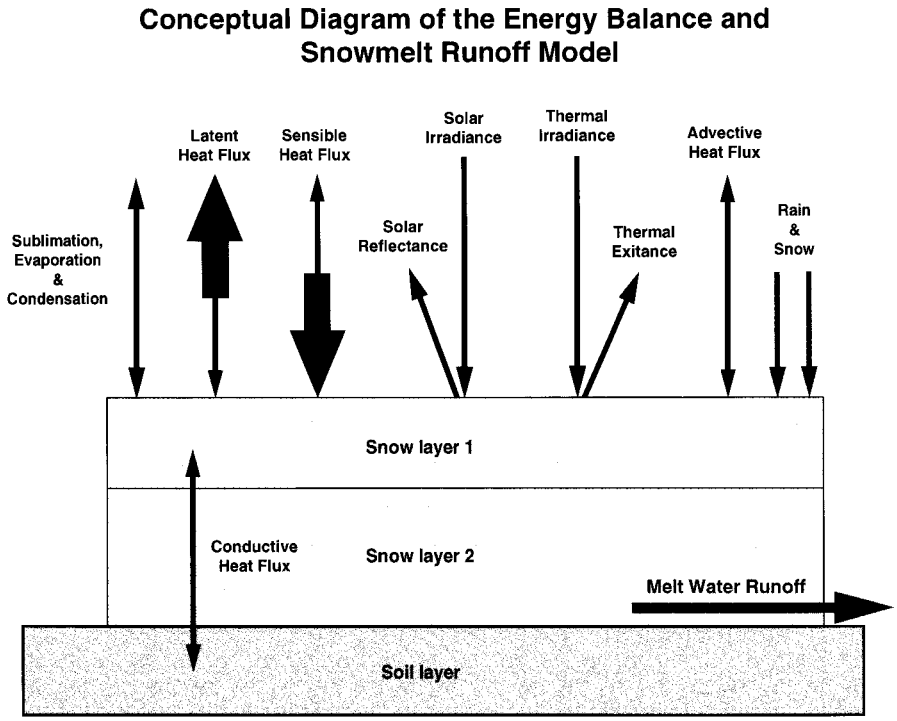

Figure 1. Conceptual diagram of the ISNOBAL energy balance snowmelt runoff model, showing the energy and mass fluxes considered and calculated at a single grid point, and the layering structure of the simulated snow cover

estimates of climate and precipitation to predict the development of, melting, and runoff from the snowcover.

The model approximates the snow cover as being composed of two layers, a surface fixed-thickness active layer and a lower layer, solving for the temperature (°C) and specific mass ($kg\,m^{-2}$) or depth of water equivalent per unit area (mm) for each.

Melt is computed in either layer when the accumulated energy exceeds the 'cold content' or when the 'cold content' is greater than 0·0. Cold content is the energy required to bring the snow cover temperature up to freezing (0°C). Runoff is estimated when the accumulated melt and liquid H_2O content exceed a specified threshold.

ISNOBAL is basically a distributed version of the point version of the model SNOBAL, though it offers fewer options. It is designed to be run over a DEM-grid of 10^4 to 10^6 cells, for an entire snow season, and is expected to complete a run in several hours, using a low-cost desktop computer workstation. The software and detailed descriptions of both models are available from Marks, Domingo, and Frew (1999).

Though ISNOBAL is a grid-based model, the point version (SNOBAL) solves the identical set of equations, and uses the same subroutine library. A detailed description of the point model structure and equations solved is presented by Marks *et al.* (1998). Figure 1 is a schematic diagram of the model structure at a point. In ISNOBAL, this structure is repeated at every grid cell within the solution region of the DEM grid for every time-step of the model run.

Model inputs

All inputs to the model are images which exactly replicate the coordinate system and spacing of DEM-grid which defines the region over which the model is run. Within this region, a mask may be input which defines a solution sub-region within the DEM-grid.

Constants. The following are set at the start, and are then assumed constant over the solution region of the DEM-grid for the duration of the run:

$\max_{z,s0}$ = Thickness of the active (surface) snowcover layer (m)
z_u = Height above the ground of the wind speed estimate (m)
z_T = Height above the ground of the air temperature and vapor pressure estimate (m)
z_g = Depth of soil temperature estimate (m)

Initial conditions. Initial conditions are specified by a seven-band image which define the DEM-grid elevations and initial snow properties.
Initial Conditions image (7-band):

z = elevation (m)
z_0 = roughness length (m)
z_s = total snowcover depth (m)
ρ = average snowcover density (kg m^{-3})
$T_{s,0}$ = active snow layer temperature (°C)
T_s = average snowcover temperature (°C)
w_c = percentage of liquid H_2O saturation (relative water content, i.e., ratio of water in snowcover to water that snowcover could hold at saturation)

Precipitation. Precipitation data are defined by a four-band image, per event, which includes the information required to calculate advected heat (from rain or snow, or both) that is added or lost during the event, and to update the specific mass of the snow cover. Rain either is translated directly to runoff (if there is little or no snow, or if the snowcover is saturated) or is added to the liquid water content.

Precipitation image (four-band):

m_{pp} = total precipitation mass (kg m^{-2} or mm)
% snow = percentage of precipitation mass that was snow (0 to 1·0)
ρ_{pp} = density of snow portion of the precipitation (kg m^{-3})
T_{pp} = average precipitation temperature (°C) (from dew point temperature if available, or can be estimated from air temperature during storm, or from minimum daily temperature on the day of the storm)

The model will parse mixed rain/snow events. It is designed to accept inputs that could be derived from typical NRCS Snotel data such as total precipitation, snow mass increase, and temperature. Average density and percentage of snow must be estimated. Rain densities are always set to 1·0. The model makes the following assumptions about the snow temperature, rain temperature, and liquid water saturation of the new snow:

when 0·0 < % snow < 1·0, (a mixed rain/snow event)

snow temperature	= 0·0
rain temperature	= 0·0 or T_{pp}, which ever is greater
liquid H_2O saturation	= 100%

Table I. Temperature-density-percent show relationship

Precipitation temperature (°C)					% snow	Snow density (kg m^{-3})
		T_{pp}	<	−5·0 °C	100%	75
−5·0 °C	⩽	T_{pp}	<	−3·0 °C	100%	100
−3·0 °C	⩽	T_{pp}	<	−1·5 °C	100%	150
−1·5 °C	⩽	T_{pp}	<	−0·5 °C	100%	175
−0·5 °C	⩽	T_{pp}	<	0·0 °C	75%	200
0·0 °C	⩽	T_{pp}	<	0·5 °C	25%	250
0·5 °C	⩽	T_{pp}			0%	0

when % snow = 1·0 and $T_{pp} \geqslant 0{\cdot}0$, (a warm snow-only event)

snow temperature = 0·0

% liquid H_2O saturation = 100%

when % snow = 1·0 and $T_{pp} < 0{\cdot}0$, (a cold snow event)

snow temperature = T_{pp}

% liquid H_2O saturation = 0%

The percentage of the mass that is snow and the density of that snow is calculated based on the given precipitation temperature. While the user may define the temperature-density-percentage of snow relationship, the default relationship is shown in Table I.

Input forcing data. Input data for climate conditions at each time step are required to drive the model. These data may be measured, simulated, or estimated, and are independent of the model. A detailed description of the methods used to estimate these parameters over a DEM-grid is presented by Susong *et al*. (1999, this issue).

Input Climate image (6-band):

I_{lw} = incoming thermal (long-wave) radiation (W m^{-2})

T_a = air temperature (°C)

e_a = vapor pressure (Pa)

u = wind speed (m s^{-1})

T_g = soil temperature (°C)

S_n = net solar radiation (W m^{-2})

If there is no solar radiation (the sun is 'down'), the last band may be omitted.

Model time steps

Two time steps are used to control the frequency of model inputs, calculations, and out-puts. The 'data time-step' is the time interval between the input climate data records. The model assumes that this interval is constant. Because the snowcover energy balance is very sensitive to diurnal variations in climate (radiation, temperature, etc.), the 'data time-step' must be 360 minutes (six hours) or less. Best results are achieved with a data time-step of 180 minutes (three hours) or less. Data time-steps greater than 60 minutes must be multiples of whole hours (e.g., 120 minutes, or 180 minutes).

The 'run time-step' is the internal time-step over which model calculations are made. Because input values are assumed to be averages over a data time-step, the run time-step is always 60 minutes (one hour) or less.

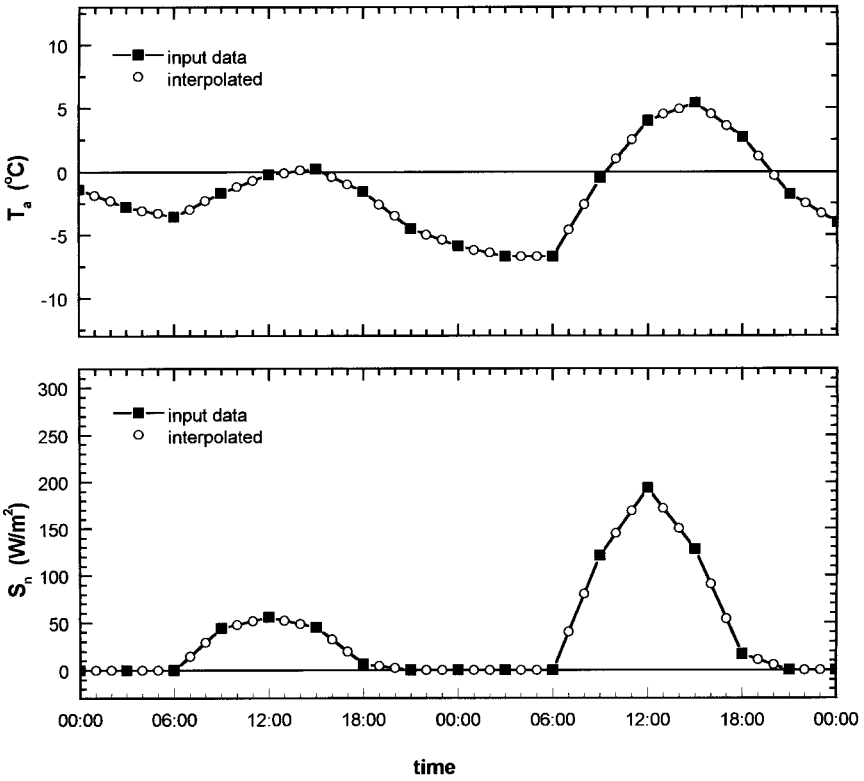

Figure 2. To achieve a stable energy balance solution, the maximum run time-step is one hour. Generation of data over a large grid at this time-step is many times impractical, so the model will allow the data time-step to be different from the run time-step, filling the intermediate values by simple linear interpolation

Figure 2 shows how the model uses simple linear interpolation to generate values for energy balance calculations at an hourly run time-step from inputs at a three-hour data time-step.

Solution instabilities occur when the run time-step is too long to account for rapid changes in the EB (e.g., sun rise or sunset), or when a layer's mass is too small to accommodate the assumption of an average flux over the run time-step.

There are three lengths of run time-steps: 'normal', 'medium', and 'small'. By default, the model uses the normal run time-step which is the longest of the three. The normal time-step must divide evenly into the data time-step (i.e., the data time-step is an integer multiple of the normal run time-step). The input data for a normal run time-step (climate data and some precipitation values) are computed from the input records by linear interpolation (see Figure 2).

The shorter run time-steps (medium and small) are used to insure solution stability. Figure 3 shows how sensitive the energy balance solution is to longer run time-steps and very thin layers. These sensitivities occur both when the model transitions from one layer to two (when the lower layer gets very thin), and when the snowcover finally disappears. The problem is solved by setting mass thresholds, below which the run time-step is switched from normal to medium, and then to small.

There are three mass thresholds for normal, medium, and small run time-steps. While these can be set, the default thresholds generally provide a stable solution. When a layer's mass falls below the threshold for the small run time-step, the model adds that mass to the remaining layer or adds it to that time-step's runoff, and removes the layer. Default thresholds are 60 kg m^{-2} (60 mm SWE) for the normal time-step,

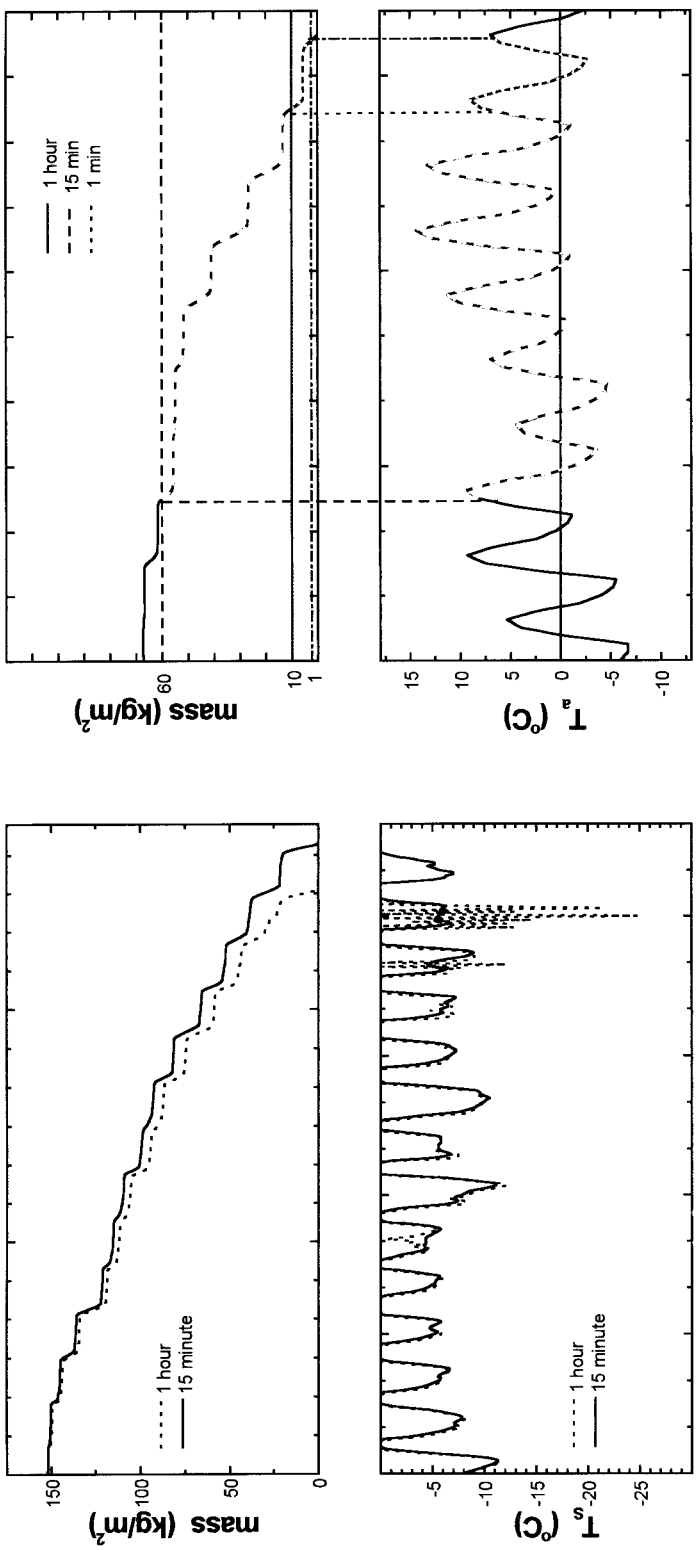

Figure 3. Illustration of how the energy balance calculation becomes unstable when the layer thicknesses are small and energy fluxes are averaged over long time periods. This is overcome by reducing the time-step. The computational requirements of this solution are decreased by instituting a variable time-step, dependent on the mass at each grid cell, over the grid

10 kg m^{-2} (10 mm SWE) for the medium run time-step, and 1 kg m^{-2} (1 mm) SWE) for the small run time-step.

Just as the normal run time-step divides evenly into the data time-step, each of the two shorter run time-steps must divide evenly into the next larger run time-step (medium into normal, small into medium). And like the normal time-steps, and as shown in Figure 3, the input data for medium and small time-steps are linearly interpolated from the input records.

All run time-step adjustment is grid-cell dependent. Only those cells which have reached a mass threshold will be run at the shorter run time-steps. This allows the model to reach a stable solution in a reasonable length of time, even over thin, low density snowcovers, such as those found in boreal or rangeland environments (see Link, 1998; Link *et al.*, this issue).

Model output

The model outputs a ten-band energy and mass flux image, and a nine-band snow conditions image. By default the model will output only one pair of these images at the end of the run. However, the model can be set to write output records at any interval up to the data time-step (one output image pair per input image). Typically, however, output is generated at a lower frequency than input. For example, if the input data time-step is three hours (180 minutes), and the run is for 210 days, then the output interval might be set to daily (one pair of output images for every eight input images).

In the energy and mass flux output image, the energy flux parameters are averaged over the number of run time-steps between output images, but the mass fluxes are summed over the number of run time-steps. The cold content (cc_s) represents the value at the time the output image is written.

Energy and Mass Flux image (ten-band):

R_n = average net all-wave radiation (W m^{-2})

H = average sensible heat transfer (W m^{-2})

L_vE = average latent heat exchange (W m^{-2})

G = average snow/soil heat exchange (W m^{-2})

M = average advected heat from precipitation (W m^{-2})

ΔQ = average sum of EB terms for snowcover (W m^{-2})

E_s = total evaporation (kg m^{-2})

q_{melt} = total snowmelt (kg m^{-2})

q_{out} = total runoff (kg, or mm m^{-2})

cc_s = snowcover cold content (energy required to bring the snowcover temperature to 273·16 K) (J m^{-2})

In the snow conditions output image all parameters represent the predicted state of the snowcover at the time the output image is written.

Snow Conditions image (nine-band):

z_s = predicted thickness of the snowcover (m)

ρ = predicted average snow density (kg m^{-3})

m_s = predicted specific mass of the snowcover (kg m^{-2})

w_s = predicted mass of liquid water in the snowcover (kg m^{-2})

$T_{s,0}$ = predicted temperature of the surface layer (°C)

$T_{s,l}$ = predicted temperature of the lower layer (°C)

T_s = predicted temperature of the snowcover (°C)

$z_{s,l}$ = predicted thickness of the lower layer (m)

w_{sat} = predicted percentage of liquid water saturation of the snowcover

MODEL APPLICATION

The spatially distributed model ISNOBAL has been applied to three basins in the western US. The tests were run in 1992, 1994, and 1996, on data from the Emerald Lake basin in California, the Boise River basin in Idaho, and the Park City area in Utah, respectively. Each site was represented by a DEM containing between 30 000 and 85 000 grid-cells, at a spatial resolution of 5 m (Emerald Lake), 250 m (Boise River), and 75 m (Park City).

All tests were run on what was, at the time, a state-of-the-art desktop computer workstation. These were not top of the line, nor were they the most expensive, but rather represented what was typical of workstations in use at the time by most scientists for modeling, GIS, and remote sensing applications. Our criteria for the limits of CPU performance was that each of the simulations had to be able to reach completion overnight, so that multiple runs were possible. Our criteria for data storage capabilities was that all input, output, initial condition, and ancillary files should fit easily on what would be considered a 'standard', or common disk drive for that time.

For these three tests, we used a Sun Sparc-2, with a dedicated 200 Mbyte disk drive in 1992, a Sun Sparc-10, with a dedicated 1 Gbyte disk drive in 1994, and a Sun Sparc Ultra-170, with a dedicated 4·5 Gbyte disk drive in 1996. The Sparc-10 was roughly five times faster than the Sparc-2, and the Ultra-170 is roughly ten times faster than the Sparc-10. The cost of these systems has been steadily falling, such that the Ultra-170 in 1996 cost approximately half what the Sparc-2 did in 1991. (Specific types of hardware are mentioned as a frame of reference only. No endorsement of specific types of hardware is implied or intended.)

Emerald Lake basin, Spring, 1986. The first test was over the Emerald Lake basin in the southern Sierra Nevada mountains of California. This basin was the site of a large water quality study from 1985–1987 (see Dozier *et al*., 1988). The basin is a small alpine cirque, just over 1 km^2 in area (see Table II). For the simulation, the site was represented by a 5 m DEM, containing 48 048 grid cells. Figure 4 shows a shaded relief image of the Emerald Lake DEM with locations of the climate stations and stream gaging station. During the period of the study it was extensively instrumented for monitoring climate and discharge throughout the year. The basin is essentially devoid of vegetation and soil. For the test, it was considered to be effectively a granite lysimeter during snowmelt, such that discharge from the outflow would respond almost directly to any runoff generated in the basin during a particular day.

Using data from spring 1986, the initial ISNOBAL test was conducted in 1992. Simulations were conducted for a period in early May, 1986, and a period in late May–early June, 1986. The 1986 snow season was one of the largest on record in the Sierra Nevada. In May, there was 5 to 8 m of snow (275 to 450 cm of SWE) blanketing the Emerald Lake basin.

During the first simulation period, 1–10 May, 1986, melt was just beginning in some parts of the basin. This period began with sunny conditions, but by 3 May a storm had moved in that continued during most of

Table II. Emerald Lake Watershed, Sierra Nevada, California

Location (approximate center)	Geodetic: 36° 36′N, 118° 40′W
Gaging station elevation	2800 m
Highest elevation	3416 m
Total relief	616 m
Basin area	1·25 km^2

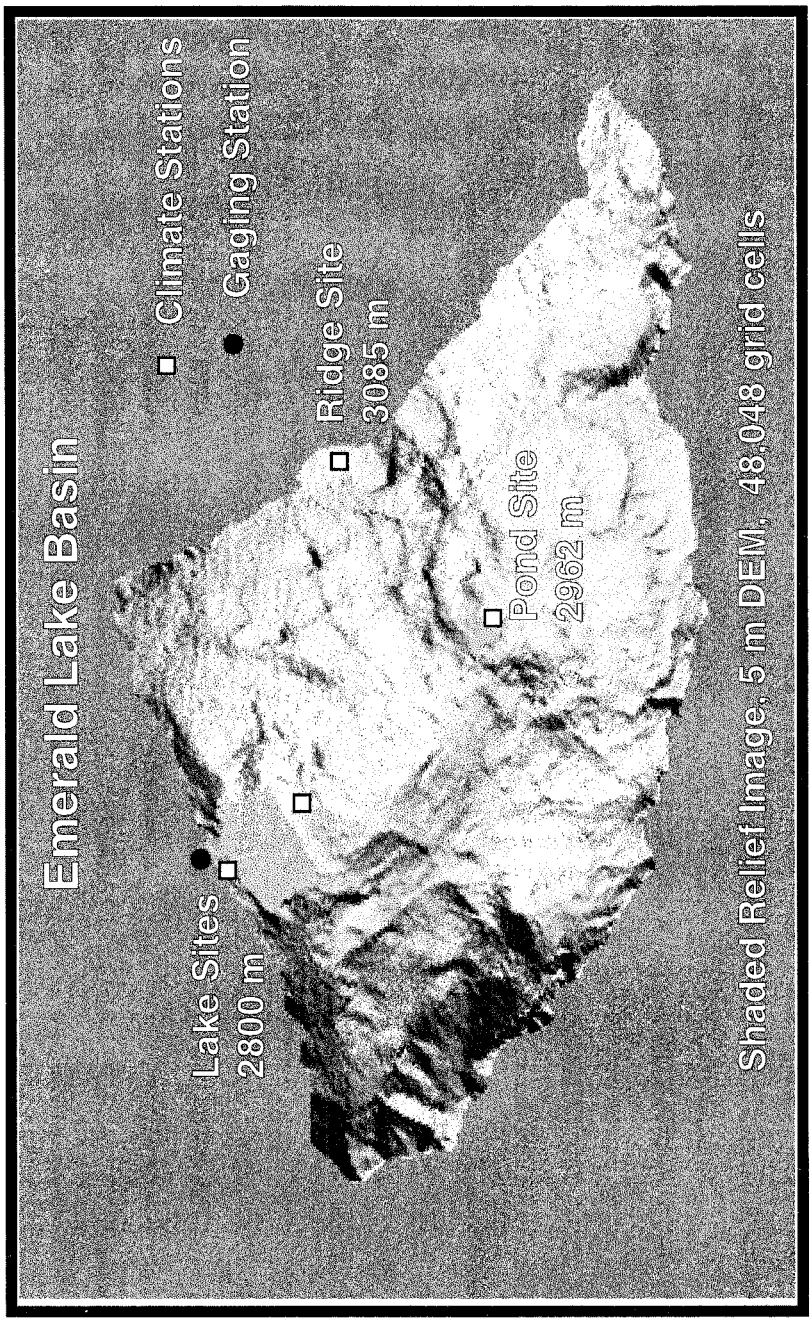

Figure 4. Shaded relief image of the 5 m DEM grid (48 048 grid cells) representing the Emerald Lake basin with location of measurement sites

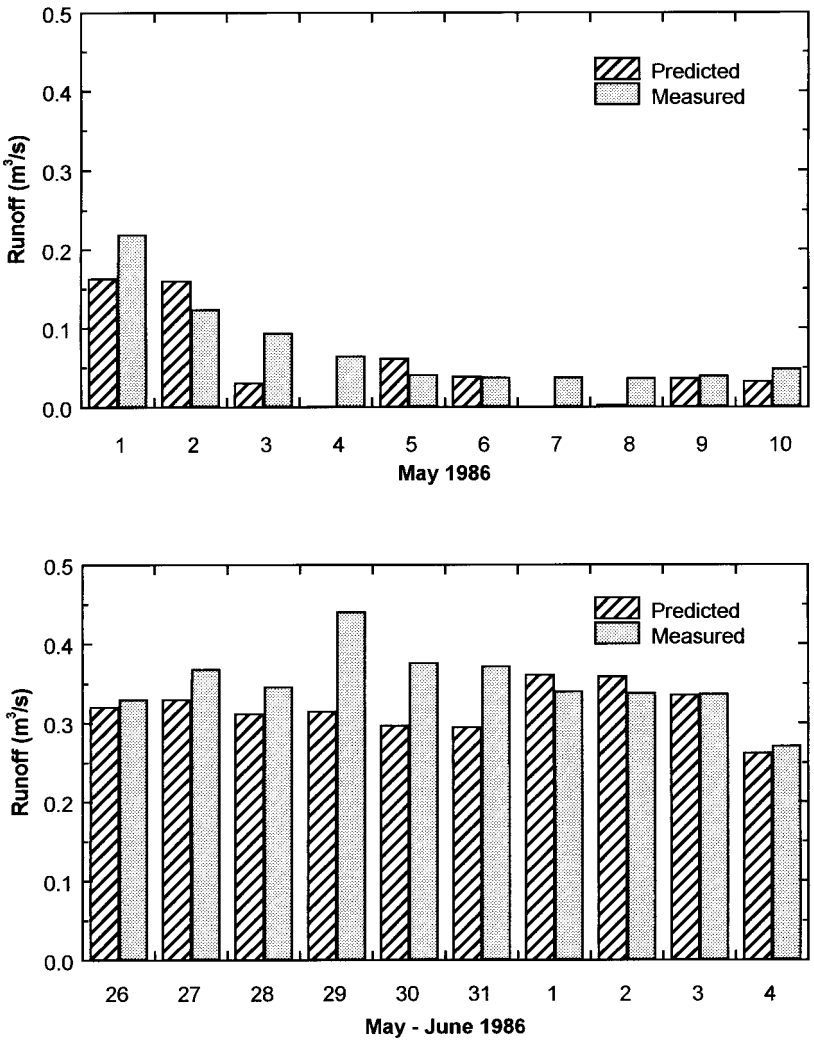

Figure 5. Measured discharge from the Emerald Lake basin for two periods during spring 1986, compared to simulated runoff from the base of the snow cover. During the first period (1–10 May 1986), a storm system came through, which generally stopped all snowmelt in the basin. The second period (26 May–4 June 1986) was sunny and warm, with active melt occurring throughout the 10 day period

the rest of the simulation. During the second simulation period, 26 May–5 June 1986, active melt was underway across the basin.

As shown in Figure 5 the simulated runoff from the snowcover in the basin closely matches discharge from the basin during both simulation periods. During the first period, melt in the basin was just beginning, with contributing areas limited to south and south-eastern exposures. The basin was covered by a deep snowcover, which had essentially been in place since a very large storm in mid-February (Marks, 1988). Grain sizes had increased, decreasing solar albedo, and allowing enough absorption of solar radiation to being the melting process (Wiscombe and Warren, 1980; Warren and Wiscombe, 1980; Marshall and Warren, 1987). However, a spring storm moved in on the evening of 2 May 1986, depositing a few centimeters of snow. This increased the albedo of all slopes, decreasing net solar radiation, and thereby eliminating melt and runoff for the rest of the simulation period.

While simulated snowmelt generally matched measured runoff from the basin during the second simulation period, 26 May–5 June 1986, there were three days (29 May–1 June) when discharge increased at

Table III. Boise River basin, southern Idaho

Location (approximate center)	Geodetic: 43° 57′N, 115° 17′W
Gaging station elevation	1000 m
Highest elevation	3200 m
Total relief	2200 m
Basin area	2151 km^2

a time when simulated melt was essentially steady (see Figure 5). This probably reflects the buffering effect that Emerald Lake itself (which was covered with 2–3 m of melting and collapsing ice at the time) had on discharge measured at its outflow. It could also reflect limitations of the assumption that the basin is effectively a granite lysimeter.

This test was run with a data time-step of one hour, and an input time-step of three hours. It required 70 Mbytes of input data, and generated 100 Mbytes of output data, and took 9·5 hours of cpu time on a Sun Sparc-2, for each simulation run. The test was close to the limit, in terms of CPU capacity and data storage, of what could be done effectively on what was, at the time, a standard desk-top workstation.

The results were encouraging, because not only did simulated melt track measured runoff, but the model showed how sensitive the melt process is to changes in climate conditions. It also showed the limitations of comparing basin discharge to simulated snowmelt. This is fairly effective in a small basin, such as Emerald Lake, but would not be in larger basins, and it would not work if the basin were partially snow-covered. Convincing verification of the model would require a direct measure of snowcover development and depletion. To test the model effectively, it would have to be run for time periods of longer than a few days, and probably over a larger basin which would include more variability in snowcover and climate conditions.

Boise River basin, April, 1990. The second test was over the Boise River basin, in southwestern Idaho. The basin has an area of 2151 km^2, and is the primary source of water for the city of Boise and surrounding communities, before flowing into the Snake River. The basin ranges in elevation from 1000 m to 3200 m, and contains six NRCS Snotel stations, where snow and climate parameters are monitored (see Table III). For this simulation test, the basin was represented by a 250 m DEM, containing 34 411 grid-cells. Figure 6 shows a shaded relief image of the Boise River basin DEM with locations of the NRCS Snotel sites and the outflow gaging station.

The basin is complex, partially forested, with reservoirs that control streamflow. While the basin may be completely snow-covered, especially following a major storm, it is much more common for it to be partially snow-covered, especially during spring. It is also common for storm events to vary over the basin, with rain in some areas, snow in others, and perhaps no precipitation at all in others.

Using data from April, 1990, this ISNOBAL test was conducted in 1994. The simulation was conducted for a 30-day period beginning 1 April 1990. This period included several storms, as well as periods of active melt over some, or all of the basin.

Input data were generated using methods described by Susong *et al.* (1999, this issue), which were based on techniques described by Garen *et al.* (1994), and Garen (1995). At the start of the simulation, the basin was extensively snow-covered, with only the lower elevations and south-facing slopes snow-free. While precipitation and air temperature data from the six NRCS Snotel sites within the basin were used along with climate data from other sources to develop the forcing data required to the model, the SWE data from the Snotel snow pillows were used only to verify the simulation.

In Figure 7, a comparison of simulated and measured snowcover mass (SWE) at the Snotel sites is presented. Though these sites are all within the mid-portion of the snow zone in the basin, they do represent a range of elevations (1600–2400 m), topographic structure, and site conditions. The process of locating the DEM grid-cell which contains a particular Snotel site is more difficult, and more critical, at some sites than others. Jackson Peak is located at the crest of gently rounded pass, and Atlanta Summit is located in the

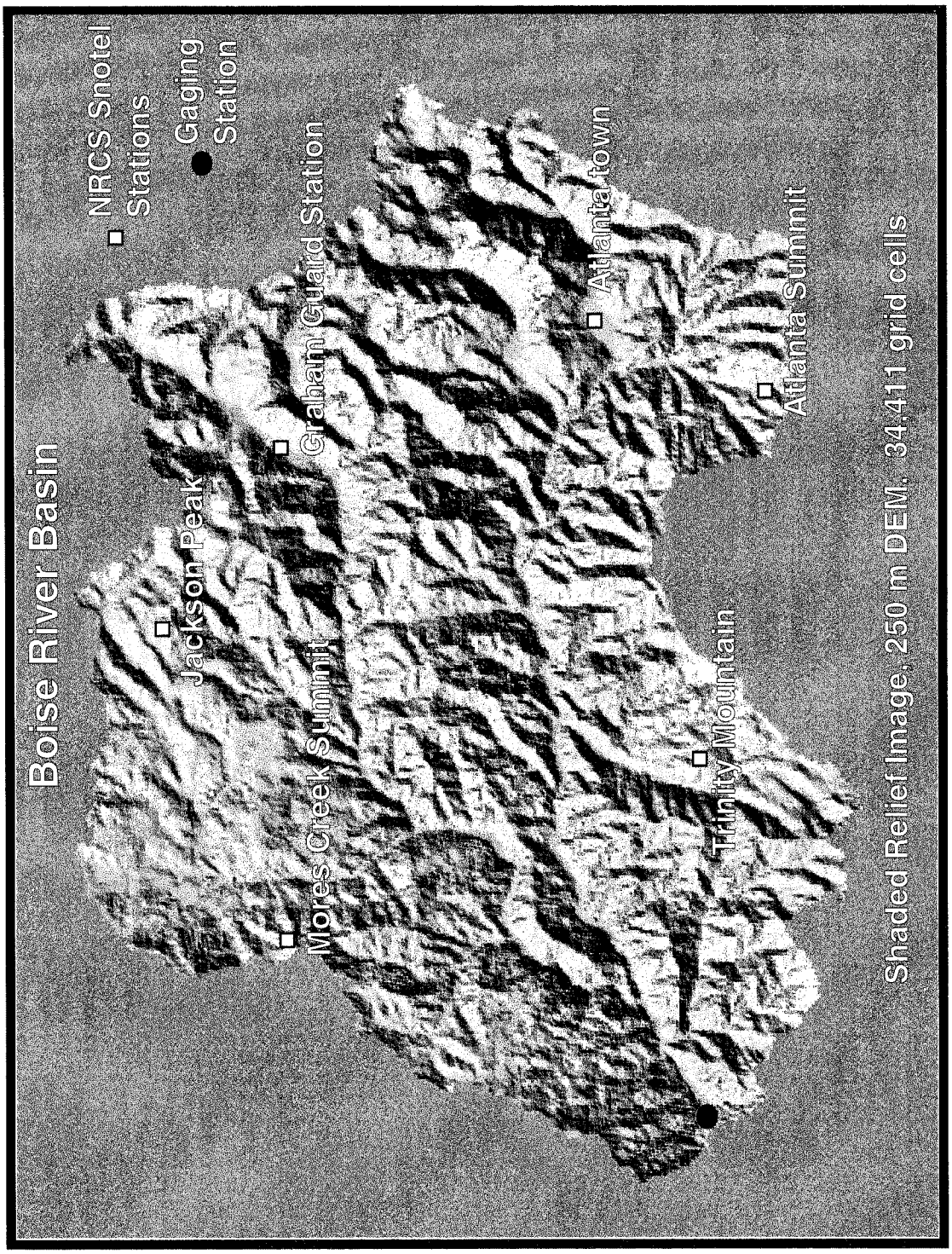

Figure 6. Shaded relief image of the 250 m DEM grid (34 411 cells) representing the Boise River basin with location of measurement sites

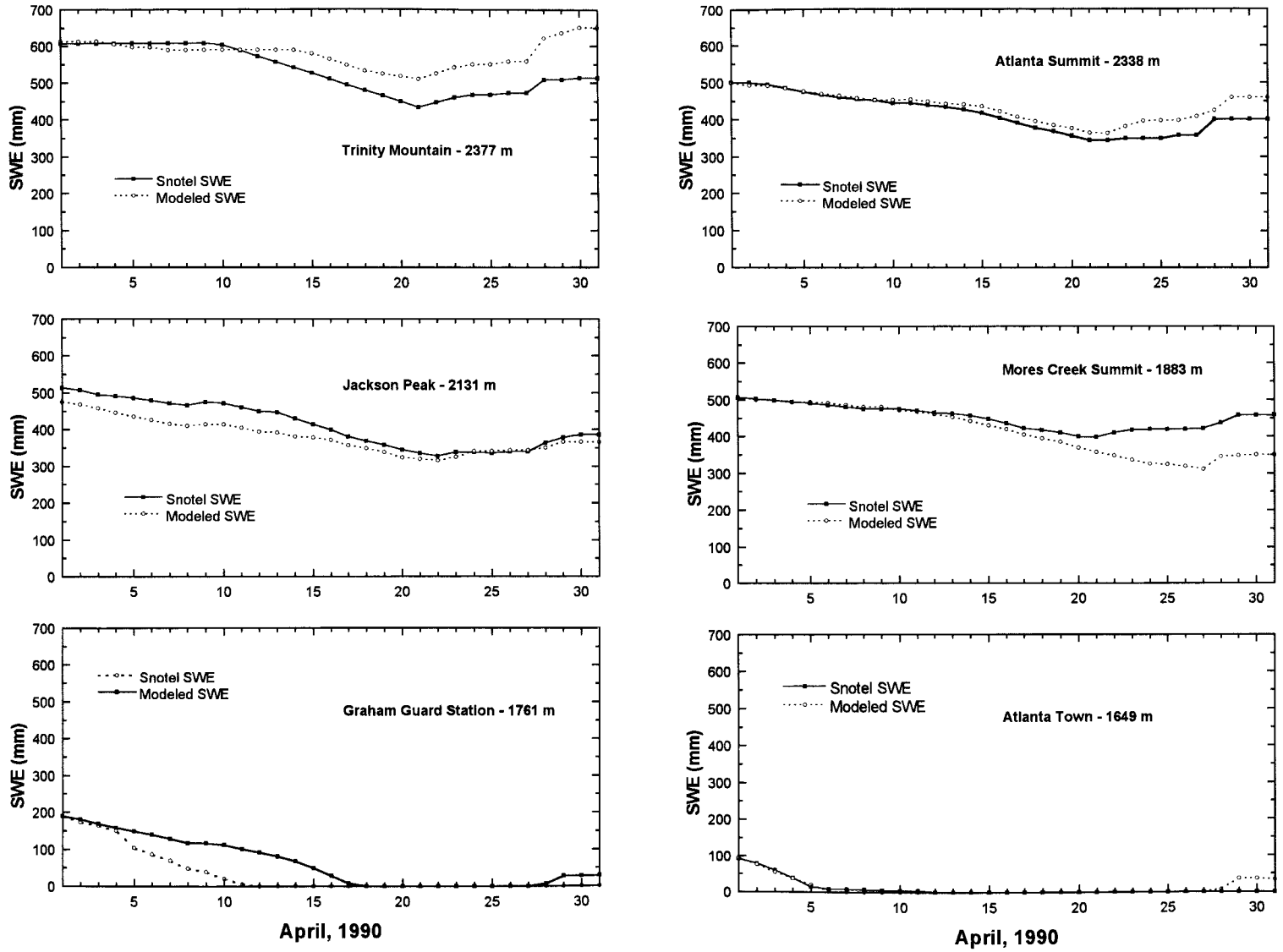

Figure 7. Measured snow water equivalent (SWE) from six NRCS Snotel sites within the Boise River basin for April, 1990, compared to simulated SWE at those sites

middle of a long, north facing slope, some distance from the actual summit. Atlanta Town is located in flat area in the canyon bottom. At all of these sites, it was straight forward to locate a DEM grid-cell which not only contained the coordinates of the Snotel site, but actually had approximately the same topographic features. At these sites, as shown in Figure 7, simulated and measured SWE are nearly identical throughout the 30-day simulation period.

Mores Creek Summit is located just over a notch in the terrain, at the divide that separates the Boise River drainage from the next basin. This site is located at the end of a long canyon, surrounded by fairly high ridges. Historically, this site has received more precipitation, and far more snowfall than would be expected for its relatively low elevation. This is probably due to a funnelling effect which draws and concentrates storms at the site, similar to that reported by Daly *et al.* (1994) regarding precipitation abundance in the Columbia River Gorge which separates Washington and Oregon. This explains why during the latter part of the simulation period, simulated SWE was declining, when measured SWE was actually increasing. The methods we used to generate precipitation did not account for this topographic anomaly, and instead estimated rain at Mores Creek during this period. Once conditions turned cold enough on 27–28 April, to assure snowfall at that elevation, both the simulated and measured SWE show a similar increase (see Figure 7).

Trinity Mountain is the highest Snotel site in the basin, and is near the crest of a ridge top. With a 250 m grid-cell size, it was very difficult to locate the DEM grid-cell which contains the Snotel site coordinates, and which matches the Snotel site topographic features. We suspect that the grid-cell selected to represent Trinity Mountain in Figure 7 was somewhat less north-facing than the actual site. This results in a slightly more rapid depletion of the snowcover from 10–21 April in the simulation, than that which was measured at the site. After that, the shape of the simulated SWE trace is nearly identical to the measured.

Graham Guard Station sits in a large, flat, meadow area surrounded by high ridges and peaks. It is frequently affected by temperature inversions, low cloud-cover, and even fog. Without solar radiation data from the site, this could not be accounted for. We suspect that the more rapid simulated snowcover depletion, compared to measured SWE, during the 4–10 April period, was caused by this effect.

This test was run with a data time-step of one hour, and an output time-step of six hours. It required 240 Mbytes of input data, and 360 Mbytes of output data, and took six and a half hours of CPU time on a Sun Sparc-10. As in the 1992 simulation test, this test was close to the limit, in terms CPU and data storage, of what could be done effectively on what was a standard desk-top workstation at the time.

This test showed that it was possible to run ISNOBAL over a large watershed (2151 km^2), for a reasonable length of time (30 days). The simulation included a range of climate and snowcover conditions, including active melt, partial region precipitation events, and mixed rain/snow events. It also involved simulation over a region that was only partially snow-covered. At the NRCS Snotel sites, simulated SWE closely matched measured SWE. Even at those sites where it was difficult to accurately select the DEM grid-cell which contained the Snotel site, patterns of simulated SWE matched measured SWE. The use of independently measured SWE at several locations within the basin was a convincing verification of the model.

The test did, however, illustrate the difficulties associated with locating point measurements within large grid-cells. In complex topography, it is difficult to select a large cell that is actually representative of the much smaller Snotel site. Also, the length of the simulation was still too brief to adequately represent both the development and ablation of the snowcover. An effective test of the model ISNOBAL requires simulation of a full snow season, and hopefully, multiple snow seasons. This would verify that the model is functional during both the cold, snowcover development period, during the mixed climatic conditions of early spring, and during the ablation period of late spring and early summer.

Park City area, 1994 and 1995 snow seasons. The third test was over the Park City area in the Wasatch mountains of Utah. This area, which is 460 km^2 and includes the mountains between Salt Lake City and Park City, will be the site of the 2002 Winter Olympics. It is currently one of the fastest growing areas, in terms of population, in the inter-mountain west. Water, principally from snowmelt, is a critical, and very

Table IV. Park City Test Area, Wasatch Mountains, Utah

Location (approximate center)	Geodetic: 40° 37′N, 111° 32′W
Gaging station elevation	1760 m
Highest elevation	3370 m
Total relief	1610 m
Basin area	460 km^2

limited resource. The conflicting demands of winter and summer recreation, forestry and natural resources, and the rapidly increasing urban needs require careful and extensive management of water from the Park City area.

The test area which includes Park City, Utah, extends beyond the Wasatch crest well into the mountain canyons above Salt Lake City, Utah. It ranges in elevation from 1760 m to 3370 m, and contains three NRCS Snotel sites, and three additional climate monitoring stations (see Table IV). For this test the region was represented by a 75 m DEM, containing 81 744 grid-cells. A shaded relief image of the Park City area DEM, showing locations of the NRCS Snotel Stations and the climate stations is presented in Figure 8.

The region is complex, partially forested, with a significant portion of the area above tree-line. Numerous alpine ski resorts are located within the region, including Alta, Snowbird, Park City, Deer Valley, Brighton, and Solitude. The crest of the Wasatch, which separates the Park City drainages to the east, from the Salt Lake drainages to the west, creates a significant rain-shadow effect. The area can be completely snow covered, but generally precipitation and snowfall decrease markedly as you move to the east from the high mountains. During winter nearly all precipitation falls as snow, and partial area precipitation events are common. During spring and early summer, mixed rain/snow events occur.

The Park City tests were conducted in 1996, using data from the 1994 and the 1995 snow seasons. As shown in Figure 9, 1994 was a dry, warm year, with a low snowcover that was essentially melted out by mid-May. 1995 was a wet, cool year, with a very high snowcover, with considerable spring precipitation (both snow and rain). In 1995, melt-out did not occur until late June. Figure 9 also shows that streamflow from the area is very sensitive to climate differences between low and high snow seasons. In 1994 there was almost no spring snowmelt peak from the three streams monitored in the Park City area, while in 1995 the snowmelt peaks were significant and very large. Stream discharge peak values were four to six times higher, and total discharge volume was eight to twelve times greater, in 1995 than in 1994 for the three streams monitored in the Park City area.

Test simulations were run from 1 March to 1 July, for both the 1994 and 1995 water years (124 days each year). Simulations included both the development and ablation of the snowcover. In 1994 all snow had melted by the end of June, but in 1995 some snow still remained in the highest mountains on 1 July.

The data time-step for each simulation was three hours, requiring 992 input images. At the start of both the 1994 and 1995 simulations the area was extensively snow-covered, with only the lowest elevations snow-free. Climate data from the Snotel stations and the three climate stations were used to drive the model. SWE data from the Snotel snow-pillows were not used to drive the model. Input data were generated using methods described by Susong *et al.* (1999, this issue).

Figure 10 presents a comparison of simulated to measured SWE at the three NRCS Snotel sites in the Park City region for both the 1994 and 1995 snow seasons. All three Snotel stations are high-elevation sites (2667–2844 m), though Mill D station is in a more protected location, while the Brighton and Thaynes Canyon sites are exposed to direct sun and wind. Location of DEM grid-cells containing the Snotel sites was easier because the grid-size of 75 m allowed more precision than the 250 m DEM used to represent the Boise River basin. Of the three Snotel stations, Thaynes Canyon was most difficult to locate because of its proximity to a ridge top.

As shown in Figure 10, simulated SWE traces closely follow measured values during the development of the snowcover in both years. In 1994 simulated SWE closely follows measured well into the ablation of the

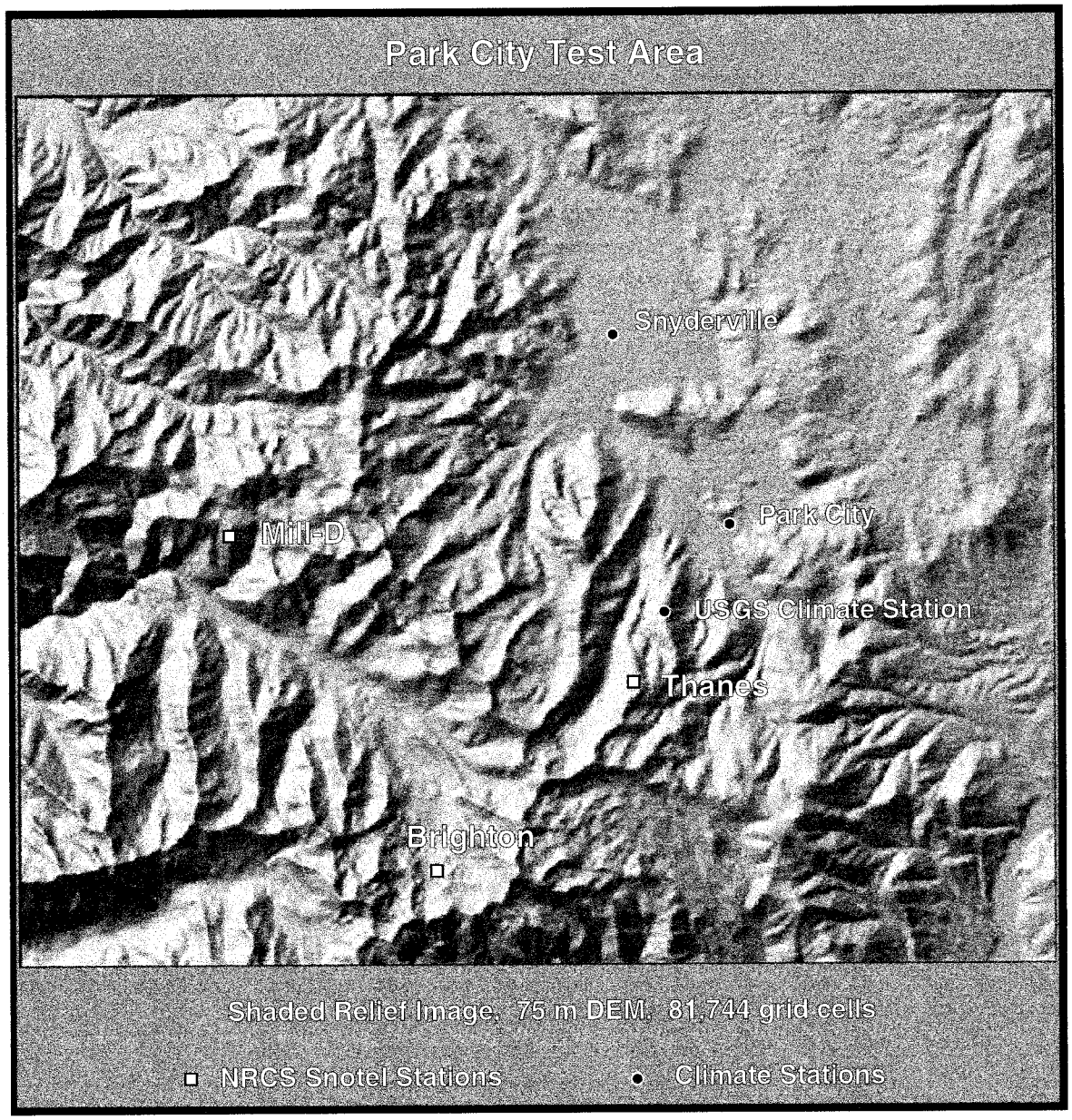

Figure 8. Shaded relief image of the 75 m DEM grid (81 744 grid cells) representing the Park City test area with location of measurement and monitoring sites

snowcover. By mid-May, late in the ablation of the snowcover, however, measured SWE declines more rapidly than simulated at the Brighton and Thaynes Canyon sites.

Solar and thermal radiation and humidity data were available through mid-May for both snow seasons from climate stations and from several of the ski areas within the Park City region. Generally, by mid-May these stations were shut down, because either the ski areas were closing for the season, or because the winter snow season had come to an end. Unfortunately, during years like 1995, significant snowcover remained, and

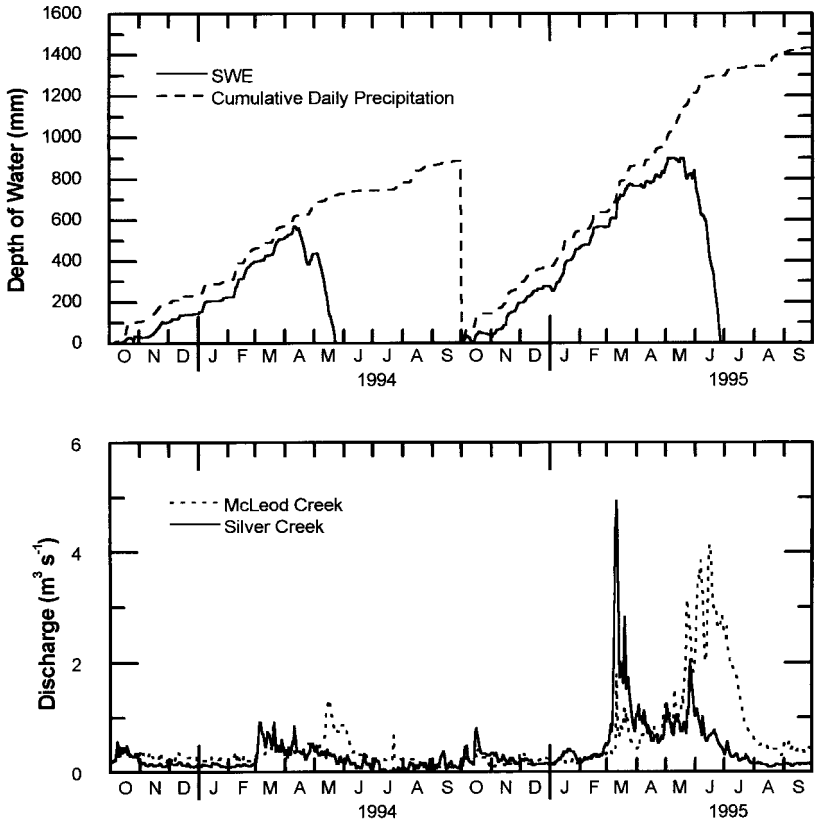

Figure 9. Cumulative precipitation and SWE from the Thaynes Canyon NRCS Snotel site, and stream discharge from two sub-basins within the Park City test area for the 1994 and 1995 water years (October, 1993, to September, 1995)

snow deposition would continue well into June. Once data were unavailable, topographic patterns of radiation were corrected for cloud cover using methods developed by Bristow and Campbell (1984) and Running *et al.* (1987). The only available humidity data after mid-May was from a low-elevation station down in Salt Lake City. During winter, there was little difference between high-elevation humidity, and humidity at this site, but during spring and summer, high elevation humidity is typically a property of the air mass, while humidity in Salt Lake City is strongly affected by local vegetation, irrigation, etc. Use of humidity from this site to extrapolate values to higher elevations tends to produce higher than expected values in the alpine zone above tree line.

May 1994 was very dry and windy. Though no data are available, sublimation was credited with the very rapid loss of snowcover during mid-May. The Brighton and Thaynes Canyon Snotel sites are exposed locations. The fact that humidity was over-estimated caused the simulated SWE during the last few days of melt-out to decline more slowly than the measured SWE. The Brighton site is the most exposed, and here we see most rapid depletion of the snowcover between 10–15 May. The Thaynes Canyon site is somewhat less exposed to wind, but we see a similar effect at this site from 12–22 May. At both of these sites, simulated SWE is not reduced as quickly. The Mill-D Snotel site was more protected from the wind than the other two sites, and we see almost no difference between simulated and measured SWE during the final weeks of melt-out (see Figure 10).

May and June of 1995 were cool and moist, with a significant number of both rain and snow events. The primary problem for the simulation tests during this period was the lack of solar radiation data to estimate

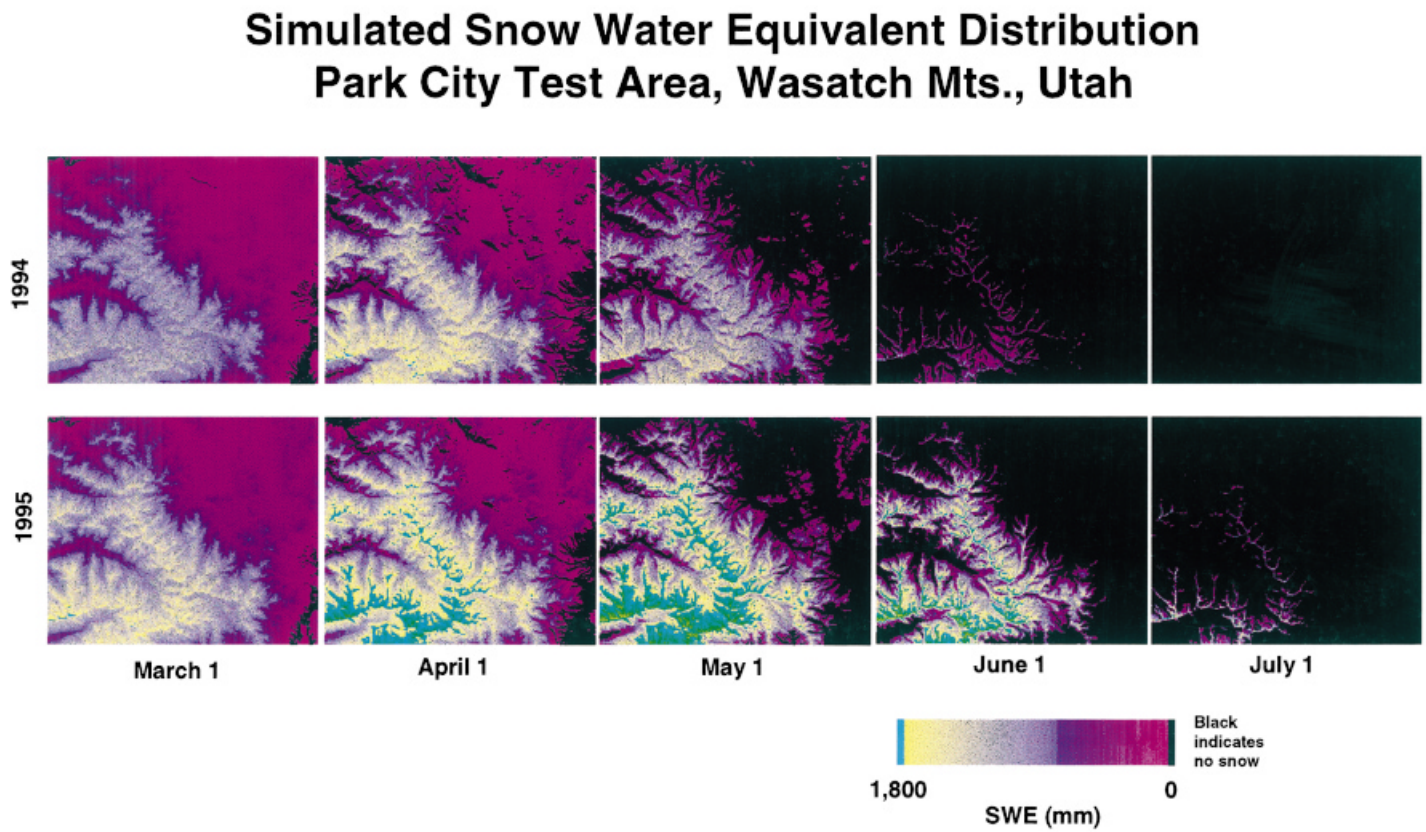

Plate 1. Simulated snow water equivalent (SWE) distribution over the Park City test area. SWE images are over the 75 m DEM grid. Black indicates no snowcover. Note that by late in the snow season (May for 1994. June for 1995) generally only the north facing slopes and very highest elevations retain snow

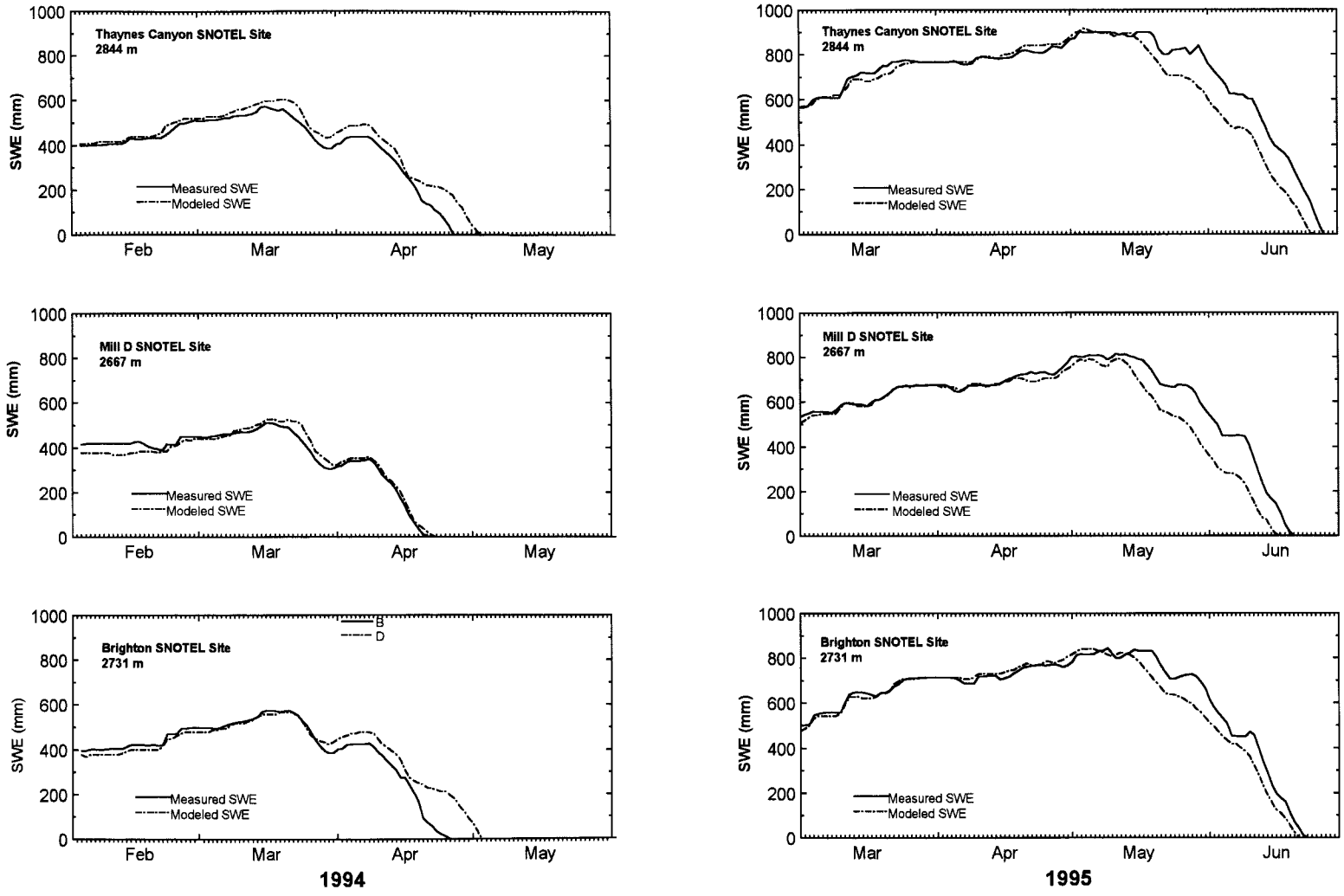

Figure 10. Measured snow water equivalent (SWE) from three NRCS Snotel sites within the Park City test area, compared to simulated SWE for the 1994 and 1995 snow seasons. 1994 was a very dry year, with a minimal snow cover that melted by early May. 1995 was a much wetter year with significant snow deposition even in May. Melt-out did not occur until mid- to late June

the actual effect of extensive periods of cloud cover. Simulated SWE traces at the Brighton and Thaynes Canyon sites generally track the measured values, though they are somewhat lower. This is probably because the estimated solar irradiance was higher than the actual values were during that period because of extensive cloud cover. Differences between simulated measured SWE are slightly larger at Thaynes Canyon and Mill-D than at Brighton. This difference was most likely caused by both shading and wind reduction caused by the vegetation canopy, which would shelter these sites and keep the snowcover cooler, allowing it to persist longer into the late spring and early summer. The Thaynes site is partially shaded by a grove of aspen trees, and the Mill-D site is much more protected by trees than either of the other sites. No effort was made to account for vegetation or canopy effects in either of these simulation tests.

Plate 1 shows a time-series of images of SWE over the Park City region during both the 1994 and 1995 snow seasons. While there is more snow in 1995 than in 1994, both simulations begin with nearly total snowcover. In both years, by April, the lower elevations are snow-free, and by May only the mountainous areas are snow-covered. In the May, June, and (in 1995) July images you can clearly see the preferential ablation on south and west facing slopes.

Figure 11 is a graphical representation of the distribution of snow mass (SWE), and mass flux (evaporation and runoff), as a function of exposure (N, S, E, W), for both the 1994 and 1995 snow seasons. Percent snow covered area (SCA) for each exposure are also indicated. Preferential loading of north-facing slopes and preferential ablation on south-facing slopes is clearly shown. It is noteworthy that there is more SWE in the region on 1 June 1995, than there was on 1 May 1994.

The Park City area simulations were run using a three-hour data time-step, and a daily output time-step. They required 1 Gbyte of input data, generated 500 Mbytes of output data, and took 12·5 hours of CPU time on a Sun Sparc Ultra-170 for each simulation. These tests were at or close to the limit of what could be done effectively, in terms of CPU and storage capacity, on what was at the time a standard desk-top workstation.

DISCUSSION

This series of tests show how ISNOBAL was developed and how improved computer technology has made it possible for a spatially distributed model that is based on the physics of the hydrologic processes involved, such as ISNOBAL a research tool with limited application (the Emerald Lake test) to a model that can be run over large basins for entire snow seasons. The Park City tests showed that it was possible to run ISNOBAL over a large watershed for an entire snow season. The two snow seasons selected for the test simulations represented a wide range of conditions, with 1994 being a low snow year, with a warm, windy spring, and 1995 being a high snow year, with a cool, moist spring. In 1994 the snowcover was essentially gone by the end of May, while in 1995 the snowcover lasted past 1 July. Simulation of the development of the snowcover closely matched measured values at all three NRCS Snotel sites. During ablation, simulated SWE matched better at some sites than others.

The tests also illustrated some problems and some data needs for application of models like ISNOBAL. Radiation data are essential to a successful model application. Humidity data, particularly high elevation humidity data, are also important. As all the three tests presented in this manuscript have shown, and as previous point simulations (e.g. Marks *et al.*, 1998; Link and Marks, 1999a), and spatial simulations (Link and Marks, 1999b, this issue) have shown, the initiation of snowmelt, and the rate that melt will proceed is very sensitive to relatively minor changes in climate. Without data to force the simulation to account for these minor variations, critical snowcover processes will be incorrectly simulated. Vegetation cover also has a critical influence on the snowcover energy balance. None of the simulations presented in this manuscript account for canopy effects such as radiation shading, emissivity enhancement, precipitation interception, wind reduction, or temperature modification. It is critical that the next set of simulation test include adjustments for canopy effects.

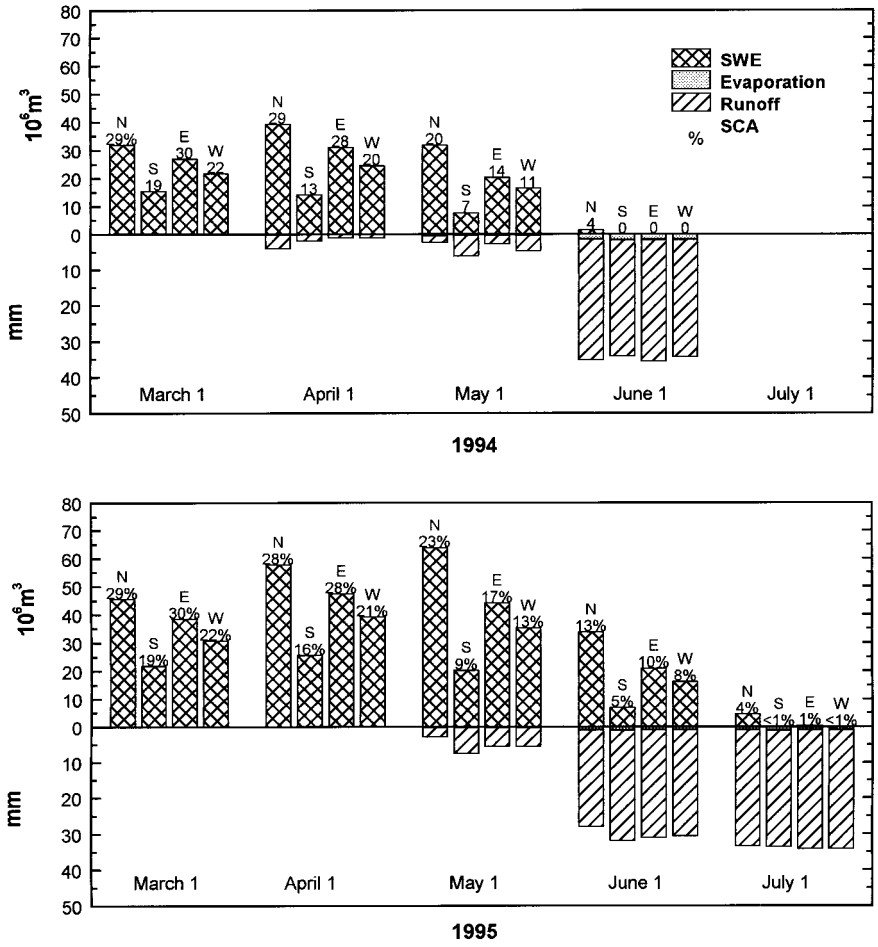

Figure 11. Distribution of SWE and mass fluxes as a function of exposure over the Park City test area for the 1994 and 1995 snow seasons. Exposures are $\pm 45°$ from the direction indicated, and flat areas are excluded. These graphs show the loading of north facing slopes during development of the snowcover during March and April, and preferential ablation of the south facing slopes during May and June

In all of the tests modelled results were compared to observed conditions that were as independent as possible. In Figure 5 observed discharge from the Emerald Lake basin is completely independent from calculated snowmelt, and in Figures 7 and 10 SWE from the Snotel snow pillow is independent from calculated snowmelt. However, for the Boise River and Park City tests, precipitation from the Snotel sites was used to drive the model, and initial snowcover conditions (snow depth, density, temperature, and liquid water content) were based, in part, on Snotel data at the start of the run. The additional initial conditions, and the input climate forcing data required to drive the model were derived either from other nearby climate station data combined with topographic adjustments, or — in the case of radiation — from models.

Three standard tests were used to evaluate model performance. The root mean square error or difference (*RMSD*) between simulated and observed parameter, and the mean bias error or difference (*MBD*) or mean deviation of simulated from the observed is presented for all three tests. The Nash-Sutcliffe coefficient or 'model efficiency' (*ME*) which describes the variation in the observed parameter accounted for by the

Table V. Mean, root mean square difference (*RMSD*), and mean bias difference (*MBD*) for the Emerald Lake and Boise River tests. Mean measured discharge, and *RMSD* and *MBD* between measured daily discharge and the sum of simulated runoff from the base of the snow cover from all grid cells for the Emerald Lake tests are presented first. (Values are reported to the nearest 0·01 $m^3 s^{-1}$.) Mean measured snow water equivalent (SWE), and *RMSD* and *MBD* between measured daily SWE and simulated SWE at the grid cell closest to the Snotel site for the Boise River test are presented second. (Values are reported to the nearest cm of SWE)

Test/Site	Mean	*RMSD*	*MBD*
Emerald Lake:			
1–10 May 1986	0·07 $m^3 s^{-1}$	0·03 $m^3 s^{-1}$	−0·01 $m^3 s^{-1}$
26 May–4 June 1986	0·32 $m^3 s^{-1}$	0·02 $m^3 s^{-1}$	−0·01 $m^3 s^{-1}$
Boise River:			
Trinity Mountain	533 cm SWE	7 cm SWE	+5 cm SWE
Jackson Peak	412 cm SWE	4 cm SWE	−3 cm SWE
Graham Guard Stn.	34 cm SWE	5 cm SWE	−3 cm SWE
Atlanta Summit	415 cm SWE	3 cm SWE	+2 cm SWE
Mores Ck. Summit	414 cm SWE	6 cm SWE	−4 cm SWE
Atlanta Town	10 cm SWE	1 cm SWE	+0 cm SWE

simulated (Nash and Sutcliffe, 1970), is presented only for the Park City test. A detailed description and a discussion of appropriate use is presented by Green and Stephenson (1986). The three tests are calculated:

$$RMSD = \frac{1}{n}\sqrt{\sum_{i=1}^{n}(x_{sim(i)} - x_{obs(i)})^2}$$

$$MBD = \frac{1}{n}\sum_{i=1}^{n}(x_{sim(i)} - x_{obs(i)})$$

$$ME = 1 - \left[\sum_{i=1}^{n}\frac{(x_{obs(i)} - x_{sim(i)})^2}{(x_{obs(i)} - x_{avg})^2}\right]$$

We chose to use these tests to illustrate the 'difference' between simulated and observed rather than the 'error', because there is a significant uncertainty in the measured parameter. It is therefore misleading to assume that a deviation from the observed is an 'error'.

From Figure 5 we can see simulated discharge from Emerald Lake basically follows the trends in measured discharge, and Table V shows that *RMSD* was small for both Emerald Lake tests, with a slightly negative bias. While the relative difference is very large for the first test (45%), both measured and modelled discharge is so small we are really at the limit of what could be reasonably measured. For most of this first test, discharge should be considered at or very close to zero. The difference is a more acceptable 7% for the second test, but while discharge is significantly higher during this period, there is little variability in measured discharge to compare simulated discharge to. Other than recognizing that the general trends of simulated discharge are following measured discharge, these tests are too brief (ten days each) to show much about overall model performance.

Figure 7 shows that simulated SWE follows the trends in measured SWE at the six Snotel sites in the Boise River basin. Table VI presents *RMSD* and *MBD* for the Snotel sites in the basin. For two of the Snotel sites, Graham Guard Station and Atlanta Town, the SWE was so low during the test (mean values of 4 cm and 1 cm SWE) that comparison against simulated is meaningful only in the sense that simulated values were also very low. For the other four Snotel sites, the relative differences range from 7–13%. The bias of this difference (*MBD*) is split between positive and negative values. The magnitude of both *RMSD* and *MBD* in all cases is small (0–7 cm SWE), and not much beyond the sensitivity of a snow pillow. For the Boise Basin test, as in the Emerald Lake test, the test is too brief (30 days), and there is too little variation to really

Table VI. Model accuracy and efficiency statistics for the Park City tests. Mean measured snow water equivalent (SWE), root mean square difference (*RMSD*), and mean bias difference (*MBD*) between daily measured SWE and simulated SWE at the grid cell closest to the Snotel sites for the Park City tests are presented. (Values are reported to the nearest cm of SWE)

SNOTEL Station	Parameter	1994	1995
Mill-D:	mean (cm SWE)	25	57
	RMSD (cm SWE)	2	8
	MBE (cm SWE)	0	−5
	ME	0·99	0·88
Thaynes:	mean (cm SWE)	32	69
	RMSD (cm SWE)	5	8
	MBE (cm SWE)	3	−5
	ME	0·95	0·86
Brighton:	mean (cm SWE)	30	60
	RMSD (cm SWE)	6	5
	MBE (cm SWE)	2	−2
	ME	0·94	0·95

evaluate model performance, other than to note that in general simulated SWE follows the measured trends at all six Snotel sites.

Figure 10 shows that for both the 1994 and 1995 snow seasons simulated SWE closely follows the trends in measured SWE at the Snotel sites, and that in general differences between simulated and measured SWE are small. Table VI verifies this, with *RMSD* values of 2–6 cm SWE in 1994 and 5–8 cm SWE in 1995. The bias of these differences (*MBD*) is about half the *RMSD*, with positive values in 1994 and negative values in 1995. The Park City tests were run for a longer period (120 days), which resulted in more variability in SWE, making the calculation of the Nash-Sutcliffe coefficient or 'model efficiency' (*ME*) appropriate. Values of *ME* varied from 0·94 to 0·99 in 1994 and from 0·86 to 0·95 in 1995, which supports the visual comparison of simulated to measured SWE in Figure 10.

The limitation of statistical tests for assessment of model performance is the basic scale problem associated with comparing a value extracted from a spatial simulation to a value measured at a point. Even if we accept the 'granite lysimeter' assumption for the Emerald Lake test, the basin is too small to provide a meaningful assessment of model performance from a water resources perspective. Runoff from a basin integrates all of the processes involved in the development and ablation of the seasonal snowcover. Even if simulated snowmelt matches measured stream-flow, that does not provide information on how well the model is simulating the patterns of snow processes over the basin.

The Snotel sites provided multiple sites across the test areas where a parameter (SWE) that was not used to drive the model was measured continuously. Though precipitation and air temperature were also measured at the Snotel sites, most of the information used to develop the forcing data for the model tests were based on a combination of terrain models and climate data from non-Snotel sites located in or near the test areas. A more robust test might eliminate the use of precipitation and air temperature data from a few Snotel sites, using these sites only for model validation. However, with only a few sites available (six for the Boise River basin, and three for the Park City area) this was not feasible.

For larger basins, such as the Boise River basin or the Park City area the Snotel sites represent areas that are much smaller than a model grid cell of 250 or 75 m. As suggested by Bloschl *et al.* (1991) a spatial measurement of the snowcover from remote sensing would be more appropriate. Unfortunately, the only remote sensing data that are routinely available are from the NOAA AVHRR instrument at a spatial resolution of 1·1 km, which is far larger than the 75 m grid used in the Park City test. Landsat TM data have a resolution of 30 m, but these data are not routinely available. Bloschl *et al.* (1991a,b) were able to get multiple estimates of snow covered area (SCA) from oblique arial photographs to evaluate performance of a

grid-based model. While this effort did show that the grid-based model performed well in comparison to more conventional snow band or parametric models, the estimates of SCA from the remote sensing data were not able to effectively track the variability of SCA during the three month period of the test. (See Figure 6, page 3187, Bloschl *et al.* (1991b.)

At a minimum, one would like a daily estimate of snow cover parameters such as SCA, snow temperature, or even the presence of liquid water in the snow at a spatial resolution close to the grid resolution of the DEM. This should be more possible with the next generation of remote sensing instruments such as MODIS (see Salomonson *et al.*, 1987) which has planned standard surface temperature and snow mapping products of 250–500 m resolution (see Klein *et al.*, 1997).

CONCLUSIONS

The energy balance snowmelt model ISNOBAL is capable of providing spatially distributed estimates of snowmelt over large complex mountainous basins. This model accurately simulates the topographic controls on snow deposition and melt, during both the development of the seasonal snow cover in winter, and the ablation of the snow cover during spring and early summer. The simulation tests presented in this manuscript show how the model was developed, and illustrate the linkage between this type of model and rapidly improving computer technology.

The simulation tests also illustrate the importance of monitoring basic climate and snowcover parameters across a full range of elevations and snow environments, and the need for high temporal and spatial resolution remote sensing data on snow cover extent and condition. The availability of radiation, humidity, and wind data in addition to the standard data on precipitation and SWE are critical to successful development, testing, and implementation of spatially distributed models such as ISNOBAL. Susong *et al.* (1999, this issue) gives a detailed discussion of methods used to generate the required forcing data, and Link and Marks (1999a, this issue) present methods used to correct climate surfaces for canopy effects. The most challenging aspects of spatially distributed modelling are in generating the climate forcing surfaces, correcting these for vegetation and canopy effects, and in developing appropriate spatial methods for model assessment.

ISNOBAL is a step toward the development of the next generation of hydrologic models. If the initial conditions and forcing data are reasonable representations of actual conditions, ISNOBAL can be used to accurately estimate the timing, magnitude, and source areas of snowmelt generation over a basin, drainage, or region. This will provide resource managers with the information required to understand the complex interaction between water and other natural resources, recreation, and changing land use, as demand for these resources increases.

REFERENCES

Anderson EA. 1976. A point energy and mass balance model of a snow cover. *NWS Technical Report 19*, National Oceanic and Atmospheric Administration: Washington, DC: 150 pp.

Anderson EA. 1979. Streamflow simulation models for use on snow covered watersheds. In *Proceedings, Modeling of Snow Cover Runoff*, Colbeck SC, Ray M (eds); US Army Cold Regions Research and Engineering Laboratory: Hanover, New Hampshire: pp. 336–351.

Bloschl G, Kirnbauer R, Gutknecht D. 1991a. Distributed snowmelt simulations in a alpine catchment: 1. Model evaluation on the basis of snow cover patterns. *Water Resources Research* **27**: 3171–3179.

Bloschl G, Kirnbauer R, Gutknecht D. 1991b. Distributed snowmelt simulations in a alpine catchment: 2. Parameter study and model predictions. *Water Resources Research* **27**: 3181–3188.

Bristow KL, Campbell GS. 1984. On the relationship between incoming solar radiation and daily maximum and minimum temperature. *Agricultural and Forest Meteorology* **31**: 159–166.

Daly C, Neilson RP, Phillips DL. 1994. A statistical-topographic model for mapping climatological precipitation over mountainous terrain. *Journal of Applied Meteorology* **33**: 140–158.

Dozer J, Melack JM, Marks D, Elder K, Kattlemann R, Williams M. 1988. Snow deposition, melt, runoff, and chemistry in a small alpine watershed, Emerald Lake basin, Sequoia National Park. *Final Report, CARB Contract A3-106-32*, Computer Systems Laboratory, University of California: Santa Barbara, CA: 367 pp.

Flerchinger GN, Cooley KR, Deng Y. 1994. Impacts of spatially and temporally varying snowmelt on subsurface flow in a mountainous watershed: 1. Snowmelt simulation. *Hydrological Sciences* **39**: 507–519.
Flerchinger FN, Saxton KE. 1989. Simultaneous heat and water model of a freezing snow-residue-soil system I. Theory and Development. *Transactions of the ASCE* **32**: 565–571.
Frew JE. 1990. *The Image Processing Workbench*. Ph.D. Thesis, Department of Geography, University of California: Santa Barbara, CA: 382 pp.
Garen D. 1995. Estimation of spatially distributed values of daily precipitation in mountainous areas. In *Proceedings of Canadian Water Resources Association Conference*, Mountain Hydrology: Peaks and Valleys in Research and Applications, Vancouver, British Columbia: pp. 237–242.
Garen D, Johnson G, Hanson C. 1994. Mean areal precipitation for daily hydrologic modeling in mountainous regions. *Water Resources Bulletin* **30**: 481–491.
Green IRA, Stephenson D. 1986. Criteria for comparison of single event models. *Hydrological Sciences Journal* **31**: 395–411.
Jordan R. 1991. Special Report 91-16, *A one-dimensional temperature model for a snow cover: Technical documentation for SNTHERM.89*. US Army Corps of Engineers Cold Regions Research and Engineering Laboratory: Hanover, New Hampshire: 49 pp.
Klein A, Hall D, Riggs G. 1997. Improving the MODIS global snow-mapping algorithm. In *1997 IEEE Geoscience and Remote Sensing Symposium (IGARSS'97)*: Singapore: pp. 619–621.
Leavesley GH, Litchy RW, Troutman MM, Saindon LG. 1983. *Precipitation-runoff modeling system: User's manual*, Water Resources Investigations Report: US Geological Survey: 207 pp.
Leavesley GH, Lumb AM, Saindon LG. 1987. *A microcomputer-based watershed-modeling and data-management system*. Proceedings, 55th Annual meeting, Western Snow Conference, Western Snow Conference, Vancouver, British Columbia, Canada: pp. 108–117.
Link T. *Seasonal Snowcover Dynamics Beneath Boreal Forest Canopies*. M.S. Thesis, Department of Geoscience, Oregon State University: Corvallis, OR: 58 pp.
Link T, Marks D. 1999. Distributed simulation of snowcover mass- and energy balance in a boreal forest. *Hydrological Processes* **13**: (in press)
Link T, Marks D. 1999. Seasonal snowcover dynamics beneath boreal forest canopies. *Journal of Geophysical Research, Atmospheres*, accepted for publication
Longley K, Jacobsen D, Marks D. 1992. *Supplement to the Image Processing Workbench (IPW): Modifications, Procedures, and Software Additions, November 1989 to June 1992 (Revision 2.0)*. Technical Report, US EPA, Environmental Research Laboratory: Corvallis, OR.
Longley K, Marks D. 1991. *Supplement to the Image Processing Workbench (IPW), Volume 1.0: Modifications, Procedures, and Software Additions November, 1989 to October, 1991*. Technical Report, US EPA Environmental Research Laboratory: Corvallis, OR.
Marks D. 1988. *Climate, energy exchange, and snowmelt in Emerald Lake watershed, Sierra Nevada*. Ph.D. Dissertation, Departments of Geography and Mechanical Engineering, University of California: Santa Barbara, CA: 158 pp.
Marks D, Domingo J, Frew J. 1999. *Software tools for hydro-climate modeling and analysis: Image Processing Workbench, ARS-USGS Version 2, Electronic Document*, [Online] ARS Technical Bulletin 99-1. Northwest Watershed Research Center, USDA Agricultural Research Service: Boise, Idaho: Available: http://www.nwrc.ars.usda.gov/ipw
Marks D, Dozier J. 1992. Climate and energy exchange at the snow surface in the alpine region of the Sierra Nevada: 2. Snow cover energy balance. *Water Resources Research* **28**: 3043–3054.
Marks D, Dozier J, Davis RE. 1992. Climate and energy exchange at the snow surface in the alpine region of the Sierra Nevada: 1. Meteorological measurements and monitoring. *Water Resources Research* **28**: 3029–3042.
Marks D, Kimball J, Tingey D, Link T. 1998. The sensitivity of snowmelt processes to climate conditions and forest cover during rain-on-snow: A study of the 1996 Pacific Northwest flood. *Hydrological Processes* **12**: 1569–1587.
Marshall SE, Warren SG. 1987. Parameterization of snow albedo for climate models. In *Large Scale Effects of Seasonal Snow Cover*, Goodison BE, Barry RG, Dozier J (eds); IAHS-AIHS Publication 166. International Association of Hydrological Sciences: Wallingford, UK: pp. 43–50.
Nash JE, Sutcliffe JV. 1970. River flow forecasting through conceptual models, Part I — A discussion of principals. *Journal of Hydrology* **10**: 282–290.
Risley J, Marks D, Link TE. 1997. Application of a quasi-energy balance model to simulate snowmelt under variable canopies during a major rain-on-snow event. *Eos, Transactions of the American Geophysical Union* **78**: F320.
Running SW, Nemani RR, Hungerford RD. 1987. Extrapolation of synoptic meteorological data in mountainous terrain and its use for simulating forest evapotranspiration and photosynthesis. *Canadian Journal of Forest Research* **17**: 472–483.
Salomonson VV, Barnes W, Montgomery H, Ostrow H. 1997. MODIS: advanced facility instrument for studies of the earth as a system. *1987 International Geoscience and Remote Sensing Symposium, I*, IEEE, New York: pp. 361–366.
Susong D, Marks D, Garen D. 1999. Methods for developing time-series climate surfaces to drive topographically distributed energy and water balance models. *Hydrological Processes* **13**: 2003–2021 (this issue).
Tarboton DG, Jackson TH, Liu JZ, Neale CMU, Cooley KR, McDonnell JJ. 1995. *A Grid Based Distributed Hydrologic Model: Testing Against Data from Reynolds Creek Experimental Watershed*, American Meteorological Society Conference on Hydrology, January 15–20, 1995: Dallas, Texas.
Tarboton DG, Luce CH. 1996. *Utah Energy Balance Snow Accumulation and Melt Model (UEB) Computer model technical description and users guide*. Utah Water Research Laboratory and USDA Forest Service Intermountain Research Station: 64 p.
Warren SG, Wiscombe WJ. 1980. A model for the spectral albedo of snow II. Snow containing atmospheric aerosols. *Journal of the Atmospheric Sciences* **37**: 2734–2745.
Wiscombe WJ, Warren SG. 1980. A model for the spectral albedo of snow I. Pure snow. *Journal of the Atmospheric Sciences* **37**: 2712–2733.

